ORIGINAL ARTICLE

Numerical Analysis for Different Masks of Car Design of High-Speed Train

B. Halfina*, Hendrato, Y.P.D.S. Depari, Muhammad, S.H.M. Kurnia and H.A. Fitri

National Research and Innovation Agency-BRIN, 15314 Indonesia

ABSTRACT – Indonesia is developing a high-speed train (HST) prototype planned for a maximum speed of 250 km/h. In high operating speed, an aerodynamics drag contributes significantly to the total resistance. Thus, reducing the aerodynamic drag becomes a primary concern. One of the significant aspects that need to be solved is to design the optimum shape of the frontal nose of the train called the Mask of Car (MoC). This research aims to study the drag coefficient from the various shape of the HST Mask of Car design by numerical method and to develop the optimum design strategy. The curvature parameters of the complex 3D model, such as nose-length, upper curvature, and side-curvature used as an optimization method The base model was constructed in 2D parameters and then developed into different shapes using 3D CAD software. A set of models was then analyzed using computational fluid dynamics with the coefficient of drag and flow characteristic. Based on the iterative simulation, it is discovered that the longer nose and sharper side of the MoC will reduce the aerodynamic drag. In conclusion, the length and the slenderness of the nose shape are significant factors in designing the mask of car of high-speed train.

INTRODUCTION

The Indonesian Government has initiated the High-Speed Train (HST) to modernize mass transit in building connectivity and mobility between cities. It is a promising alternative to the high-load air traffic, especially in the Island of Java. To support that purpose, Indonesia National Research and Innovation Agency started constructing a High-Speed Train prototype designed to have a maximum operating speed of 250 km/h. It will significantly reduce travel time between big cities, accelerating mobility and economic growth. Currently, travel time between Jakarta to Surabaya is approximately 8.5 hours, with the maximum speed reached is 120 km/h in some areas. However, in this high velocity, aerodynamic drag becomes a significant concern and must be reduced.

A bullet-shaped design is a commonly used geometry for the HST operating globally. However, some adjustments and modifications are needed before implementing the available design. A unique and customized shape design is needed to match the technical requirements and manufacturing capability in Indonesia. As an example, an extreme curvature of the windshield is less favorable due to the complex manufacturing and fabrication. Another example is the nose-tip shape of the HST must be designed to be able to house the coupling mechanism of the train.

Referring to the drag force equation, an increase in speed by a factor of two on the current operational speed will increase the aerodynamic drag by four times. Aerodynamic drag has two components: pressure and viscous drag. In the front area, there is a very high-pressure region. For a high-speed train that runs above 200 km/h, the aerodynamic drag outnumbers mechanical resistance and contributes to more than 80% of total resistance at 300 km/h [1]. According to Baker, reducing the aerodynamic drag by x% will lower fuel consumption by 0.5x% [2]. Hence, reducing aerodynamic drag is critical from a cost and performance standpoint.

The shape design and running environments serve as a significant influence on the high-speed train's aerodynamic characteristics. Nevertheless, while it is impossible to significantly change the running setting, limited by track conditions and construction costs, train design is the preferred approach for improvement [3]. To achieve minimum aerodynamic drag, the shape of the train's front nose, called the Mask of Car (MoC) must have good aerodynamic performance.

Several studies have investigated the consequence of the bullet train's front area on the aerodynamic characteristic. Kwak et al. [4] optimized the KTX Sancheon base model with the Broyden-Fletcher-Goldfarb-Shanno algorithm, resulting in a 6% reduction in aerodynamic drag. The study also found that elongating the train's nose and sharper edge shape lessens the vortices behind the tail car, thus lowering the aerodynamic drag. Choi and Kim [5] analyzed the GTX train using Computational Fluid Dynamics (CFD). The study found that changing the nose from a dull to a streamlined shape can lower the drag force by up to 50%. The curvature parameters of the complex 3D model, such as nose length, upper curvature, and side curvature used as an optimization method. The base model was constructed in 2D parameters and then developed into different shapes using 3D CAD software.

Based on the study explained, various methods exist to study train aerodynamics. CFD simulation has been extensively used. CFD analyses provide valid engineering data for conceptual design studies prior to building prototypes and physical testing. It allows the design team to quickly test the model's coefficient of drag and provides suggestions for the optimum design. In this study, a 3-cars formation model was simulated in the CFD simulation. This configuration can represent

airflow conditions in one trainset of HST. Hence, this research aims to study the drag coefficient from the various shapes of the HST Mask of Car design by numerical method and to develop the optimum design. Once the optimum design with reduced aerodynamic drag is established, the next step is to build a scaled model for the empirical experiment. A wind tunnel is a validation method for numerical simulation. It has been a proven method to study the aerodynamic phenomenon around an object. However, due to the high-cost experiment, only the optimum designs were tested.

METHODOLOGY

Geometric Model

Computational fluid dynamics is a field of computational fluid dynamics that uses computational techniques and algorithms to solve fluid flow problems. The use of computers can assist in the calculations needed to simulate the relationship between a fluid and a solid surface. Using a supercomputer can further improve the results of solving fluid flow cases. CFD is a technique that replaces integral and partial differential equations with discrete algebraic equations, allowing solutions in the form of numerical values of flow at discrete points in space and time [6],[7]. It can take tens of hours to simulate a finite element model because of having a significant degree of freedom. To decrease computational time, we should do pre-processing at the first stage of CFD simulation which is construction of simplified geometric models. The model must be simple and cleaned, while still resemble actual train and provide accurate results. The frontal shape is derived using the train shape function. To maximize the results of the analysis to focus on the frontal shape, the model is simplified where the other influencing factors are removed and then used as a simulation model. It can work by eliminating the step difference by lowering the height of the front/rear difference and widening the vehicle width [4]. In this study, CFD analysis was carried out based on the simplified cell model of a high-speed train. Figure 1 illustrates the transformation shape of the model from a 3D complex form to a solid model for simulation. The shape of the assembled parts must be simplified and emphasized into a single unit. The included bogies and wheels, along with the pantograph, were eliminated to obtain a simpler model. The simplified 2D shape of the nose as seen in Figure 2, represents curves of the nose mode.

| (a) rendered view of HST Model | (b) 3D section shape of HST Model | (c) cleaned geometry for simulation |
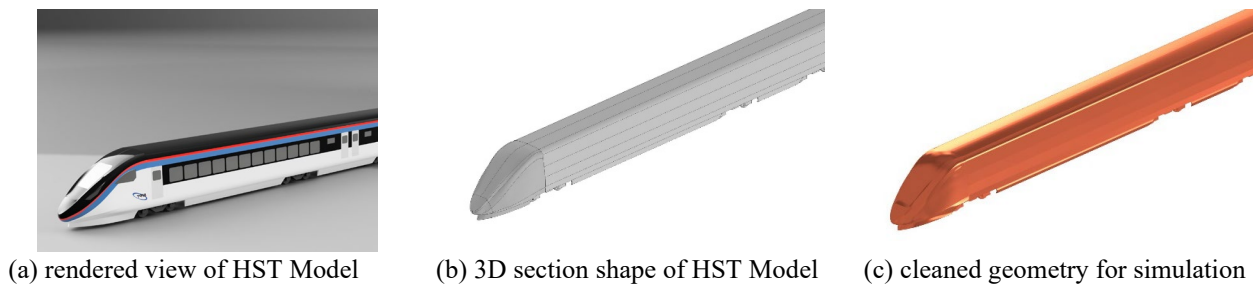
Figure 1. Forming process of HST model
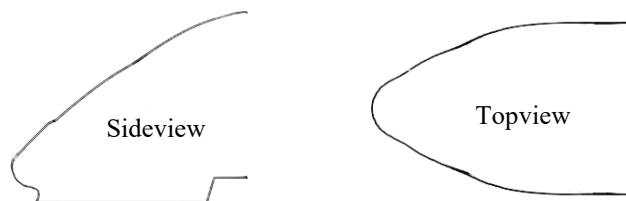
Figure 2. Sideview and topview of 2D shape

Numerical Analysis Techniques

A 3-cars arrangement of a streamlined HST prototype with a simplified bogie was applied in this study as a simulation model. The dimensions and configuration of the train model used in this study are based on the design of an Indonesian high-speed train that has been developed by the Indonesia National Research and Innovation Agency. The train model has a width (W) of 3.25 m, a height (H) of 4.05 m, and a total length (L) of 70 m, as seen in Figure 3. Since there is no space limitation as in the wind tunnel experiment, the models were built in actual size in CFD simulation. Therefore, the actual Reynolds number was used. The CFD simulation was then run on two different nose-length models [4]. CEN standard was applied to the simulation models, and streamlined area, windshield, and bogie were simplified [8],[9].

Environmental influences are crucial in the fluid flow simulation; thus, the boundary conditions need to be defined prior to the calculation. An enclosure as the simulation domain was constructed to represent the surrounding air in the actual environment. It has an inlet, outlet, and wall as boundary conditions. Train length (L) 70 m was used as a consideration of the enclosure's dimension, as illustrated in Figure 4. To simulate the complex flow around the train shape, such as the ground boundary layer, in detail. Slip resistance condition is applied, all surfaces of the train model are fixed ground conditions, and the no-slip condition is used. Only in the case of the ground surface the moving ground

condition was applied to mimic the relative motion of the ground and the train. The gap between the train model and the ground was selected as 0.2 m by adding the rail height to the distance between the train floor and the shape of the bogie wheel with reference to the EN Standards.
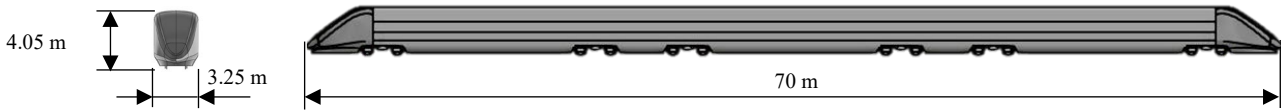
Figure 3. A 3-cars arrangement of streamlined train model
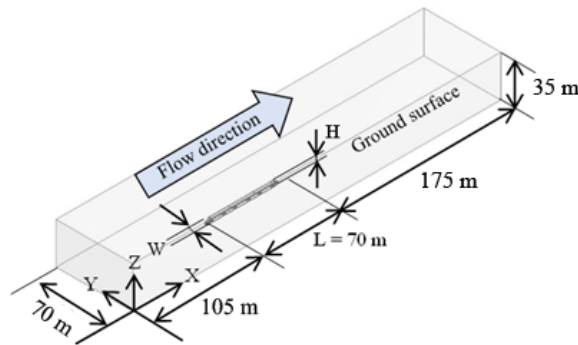
Figure 4. Dimension of the computational domain or enclosure

The boundary conditions were then defined in the simulation box. The inlet was the frontal area located at 105 m from the train nose (1.5 length of train model), while the outlet behind the tail end of the train model is defined as 175 m or 2.5 length of train model to give sufficient space for the wake vortices phenomenon to be captured. The enclosure's width is 1L or 70 m—the height is set to be 35 m (0.5L). The element size used in the meshing is 2000 mm, with the number of elements being 1,734,788 and 327,863 nodes. The detail of the mesh is shown in Figure 5. In this simulation, we considered the boundary layers at the train's surface by implementing an inflation meshing strategy. It has a total thickness of 200 mm and five layers. The vector velocities, pressure magnitude near the surface and related parameters can be observed.
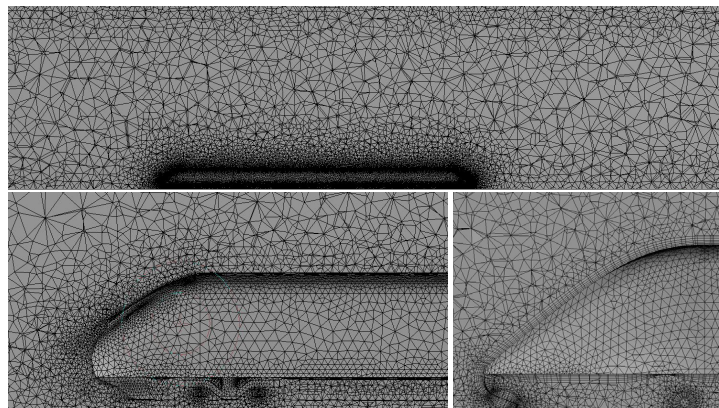
Figure 5. Detail mesh of the train model with inflation layers

Numerical analysis was performed at the target maximum operating speed of 250 km/h and a design speed of 300 km/h. The Reynolds Number calculated on the train speed of V=250 km/h, air density of 1.225 kg/m³, and the kinematic viscosity of 1.7894×10^{-5} kg/m-s is 8.33×10^{6}, meaning the flow is turbulent. The study used the three-dimensional incompressible standard k–ε model as the turbulence model derived from transport equations for the turbulence kinetic energy (k). This model has reasonable accuracy and robustness, so it is widely used in industrial and academic research. The CFD simulation calculated the solutions iteratively until achieving a convergent result. The residual is one of the primary quantitative indicators of the iterative solutions; it measures the differences of the conserved variables in the control volume. A residual is never precisely zero—however, the lower the residual value, the more numerically accurate the solution. The residual of each turbulent was at least 1×10^{-6}. As in Eq. (1) the aerodynamic drag coefficient was used for aerodynamic drag comparison, and the standard cross-sectional area was 13 m².

$$C_D = \frac{F}{\frac{1}{2}\rho V^2 A_{ref}}$$

(1)

where, C_D is the drag coefficient, F is drag force (N), ρ is the density of air (kg/m³), V is speed (m/h), and A_{ref} is the reference area (m²).

Mask of Car Design Variations

Through analysis of the basic shape of the mask of car, it is calculated that three variables significantly influence aerodynamic drag. These variables were selected based on the conditions of various commercial vehicles. The nose length and lateral curvature substantially affect the aerodynamic drag coefficient, which is the objective function; it has a dominant role in deriving the optimal shape. The length of the frontal head, the height of the tip of the frontal part, upper and lower curvatures in the lateral view, and lateral curvature in the planar view greatly influence aerodynamic drag [4]. The variables used to consider the variation of the model design in this study consisted of nose length, upper surface curvature of lateral view, and the side surface curvature of planar view. They are designed by considering the interior of the control room and the driver's eye of reference. Different types of the three models are shown in Table 1.

To get a variety of analysis results and produce a model with the desired coefficient of pressure drag, aerodynamic drag, and viscous drag, three MoC models have been developed within the range that does not disrupt the geometrical interference conditions of commercial vehicles. The model was varied by reducing the length of nose with a deviation of approximately 0.5 m. Variation of nose length is 5 m, 5.5 m, and 6 m for lower, middle, and upper models. Meanwhile, the shape transformation from the lower model to the middle model based on the upper surface curvature variable was approximated with a different angle of 13 degrees backwards to the y-axis to represent a mask of car construction that is easier to manufacture. In the upper model, the change of shape is carried out by referring to the concept of a dolphin nose. Variation of upper surface curvature is about 66, 53, and 48 degrees to the y-axis for lower, middle, and upper models. Variation of side surface curvature was based on the mask of car width, which is 2.17 m, 2.34 m, and 2.35 m for lower, middle, and upper models approximately.

Table 1. Different shapes according to variations of the design variables

Design variable	2D Shape variation	Lower Model	Mid Model	Upper Model
1. Nose Length				
2. Upper surface curvature				
3. Side surface curvature				
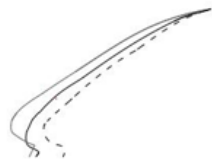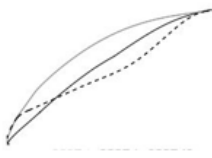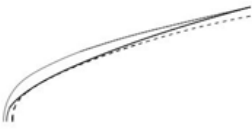
RESULTS AND DISCUSSION

Nose Length Effect

Three models of train with different nose lengths were compared. The length of the mask of car will be used as a consideration for the actual design of high-speed train, which will be built. The vortex formation was visualized using the constant Q iso-surface to explain the aerodynamics of trains [10]. The Iso-surface with q-criterion described in Figure 6 shows vortices developing from the frontal area of the train to the rear end. In the lower model or shorter nose, the region of vortices is more extensive and stronger than in the longer nose. The right-hand side of Figure 6 shows wake vortices at the tail-end of the train. Vortices are wider and dispersed to the side at the lower model. In a closer look, Figure 6 also visualizes that the vortices occur in the second car area of the shorter train. A vortex drag is the dominant element of aerodynamic drag; thus the vortices differences between head and tail of the shorter train nose results in a more significant drag than the longer train nose.
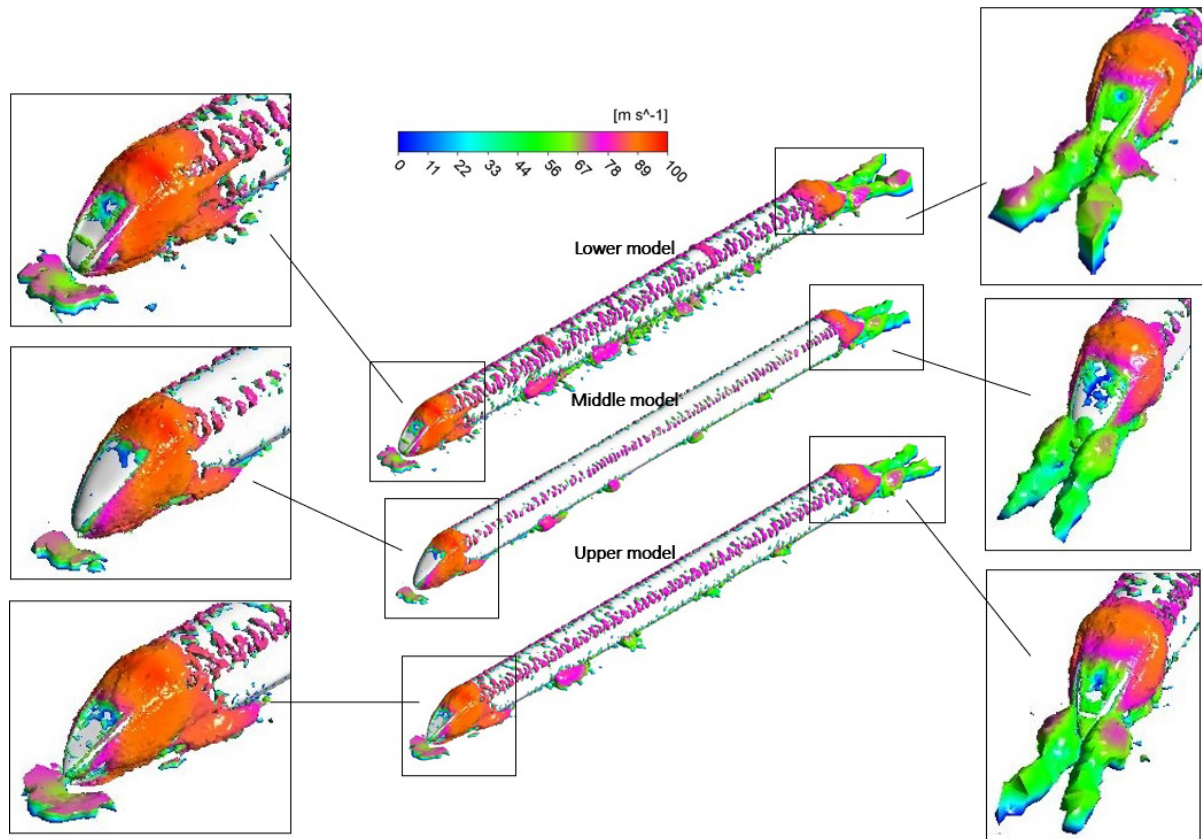
Figure 6. Vortex core region at the nose and tail-end of the train

Figure 7 shows the aerodynamic drag lower model is 0.37, the middle model is 0.363, and the upper model is 0.36. The aerodynamic drag value is relatively similar for the middle model and upper model, as the increase in length from the nose length is only 0.5 meters and has a minor effect on the aerodynamic drag. Therefore, within the range of 0.5 and 1-meter modifications in this research only reduce aerodynamic drag by just 1%. A significant reduction of the aerodynamic drag needs up to 50 % will only be possible by increasing up to 10 m [11].
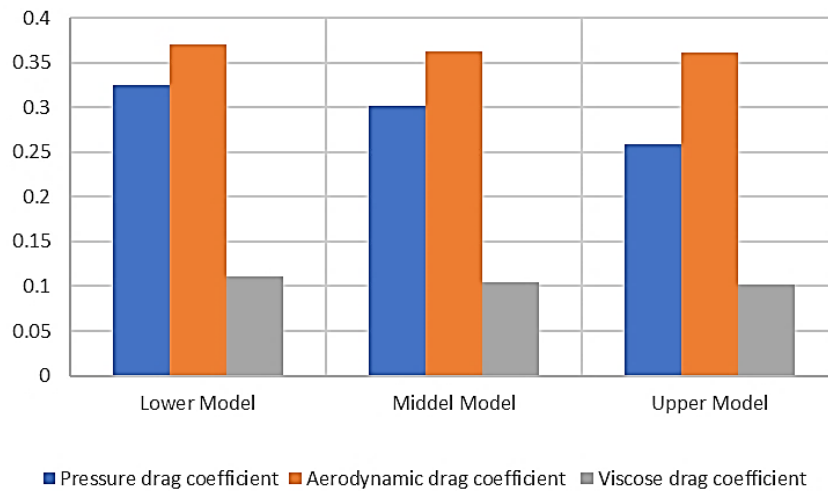
Figure 7. Comparison of drag coefficient between 3 models

Upper Curve Effect

The effect of the upper curve in MoC was analyzed using three different models representing convex, slender, and concave curves. A streamlined nose may decrease half of the aerodynamic drag compared to an obtuse train head [5]. Figure 8 illustrates the velocity vectors around different nose curves. It is observed that each vector has a different speed relative to its position at the mask of the car's face. The velocity magnitude decreased as the air struck the train head -- reaching the stagnation point at the tip of the nose. Due to the shear layer, the stream of air will follow the nose's surface, gaining its acceleration and reaching the highest speed at the top of the MoC transition to the car body. In the upper model, more low-velocity vectors occur at the tip of the nose compared to the other two models. This indicates that in the lower model, a wider surface area obstructs the air flow stream. On the other hand, the lower model has fewer low-

velocity vectors due to the narrower obstruction area. However, due to its concave curve, the airflow is inhibited from gaining acceleration. The middle model is the optimum among the others. The vector velocities transition indicates that the air streams freely to the rear of the train.
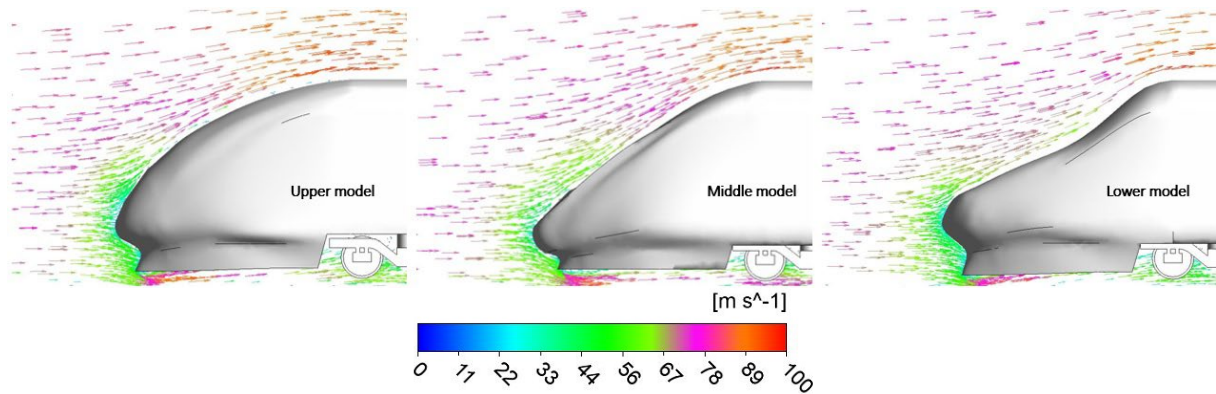
Figure 8. Velocity vectors in different upper curve
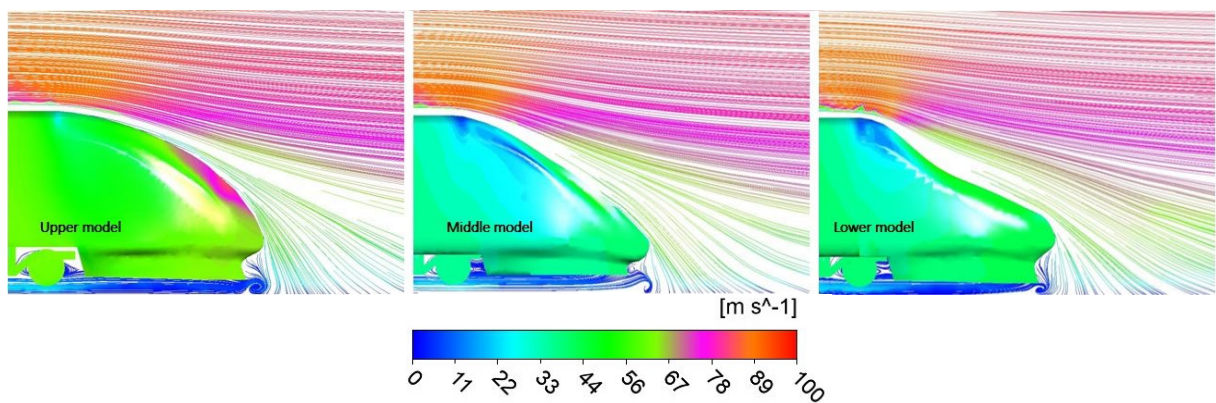
Figure 9. Velocity streamline at the tail-end of the train

Figure 9 describes the streamline and the pressure contours at the read-end of the train. The upper model has the highest-pressure concentration at the curved area, indicating low velocity at the separation zone, generating larger vortices. The figure also shows that in the upper model, separation occurs in a higher location near the roof, thus resulting in the thickness of vortices that will be generated relative to the ground. Pressure drag is one of the element in the aerodynamic drag; therefore, observing pressure contours around the frontal area helps analyze the overall aerodynamic drag of the model. The contour portrays the pressure value across the surface. Surface pressure primarily intensified at the head and tail-end of the train [12]. The previous speed vectors indicate a blue region at the nose that illustrates rapid velocity decrease or even zero. Hence, air particles became denser, inducing a rise in pressure. On the opposite, at the roof-top transition between the MoC and car body, the pressure decreased as a result of increasing flow stream upward the rear area of the train.

Naturally, the air flows from the high-pressure area to the low-pressure area on top of the MoC [13]. As seen in Figure 10, the upper model has the largest region of highest pressure shown by the red contour plot. The lower model shows the distribution of high-pressure concentration, meaning that the low-velocity region occurs not only on the tip of the nose but also at the windshield area. A lower curve and streamline of the MoC design allow air to flow freely upstream, minimizing drag. Table 2 describes the correlation between the calculated pressure drag coefficient to the aerodynamic drag coefficient.
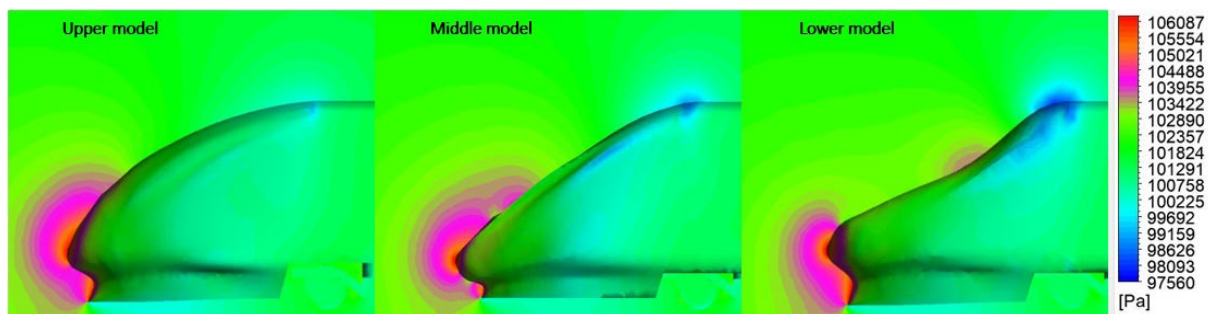
Figure 10. Pressure contour at the MoC

Table 2. Pressure drag and viscous drag coefficient of the models

No	Model	Pressure drag coefficient	Aerodynamic drag coefficient	Viscous drag coefficient
1	Lower Model	0,252	0,351	0,099
2	Middle Model	0,244	0,34	0,096
3	Upper Model	0,248	0,341	0,098

Side-Surface Effect

At the rear of the model, longitudinal vortices were formed. Contours of the velocity magnitude in the vicinity of the tail-end are shown in Figure 11 to illustrate the side surface effect on the separation of the flow. The two vortices trailing the tail-end of the train model can be observed to study the drag characteristics [4]. It can be seen from the image that there are two blue contours indicating that the separation of flow has a lower magnitude. In the lower model, the pair region of the vortex separation was wider, and the gap between the vortexes was wider. On the opposite, the distance between the eddies at the upper model is narrowed and crippled. The size of the vortex is also seen wider in the upper model and reduced narrowed in the slenderer model. The optimization aims to weaken the wake vortices [4]. These contours confirm mentioned that drag is reduced when the gap between vortices is also reduced [14][15]. Thus, the slender design showed a lesser gap between longitudinal vortices. Following the CFD simulation, an experimental test was conducted at the wind tunnel facility to validate the results as well as capture the flow visualization. Figure 12 shows the setup of the HST scaled model inside the wind tunnel chamber. However, due to the high-cost experiment, there were only two models tested. The coefficient of drag from the wind tunnel was 0.38, or a 10% difference from the numerical simulation.
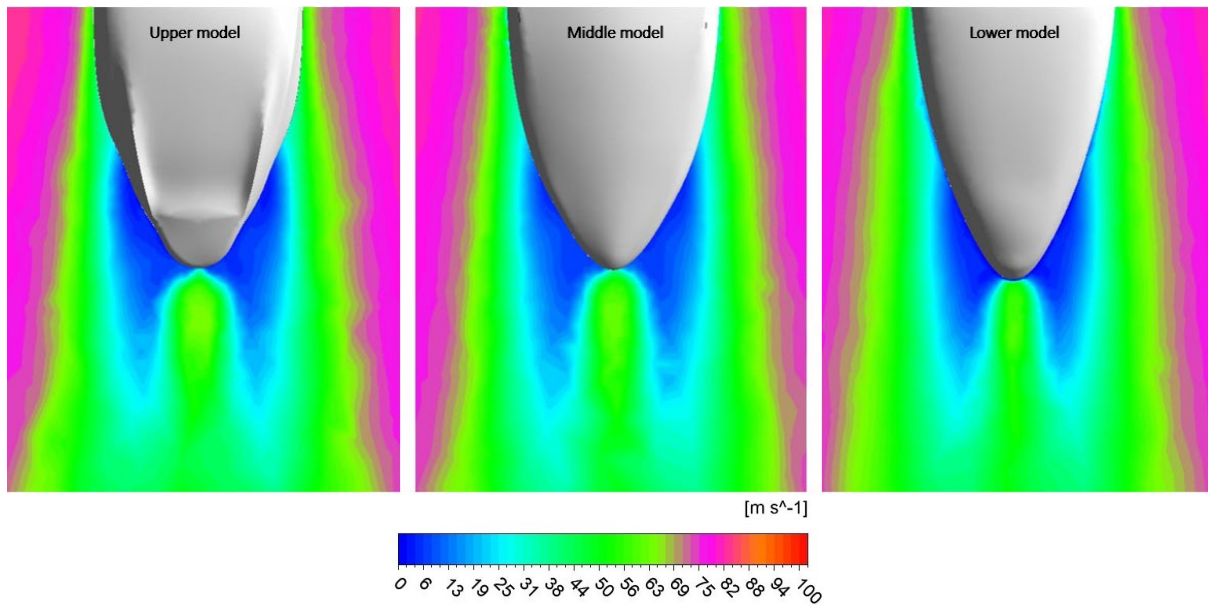
Figure 11. Velocity contour

Figure 12. Wind tunnel test of HST scaled-model

CONCLUSIONS

In this study, different shapes of the frontal area of the mask of car design were analyzed. Shape variables were characterized by three variables, nose length, upper curve, and side curve. The parameters can be used as effective guidance for design modification to get optimum design during the HST development stage. The nose length affects the area and the strength of the vortices generated during HST movement. The CFD simulation found that the additional length of the nose to the model is insufficient to reduce the coefficient of drag. Additional length up to 1 meter only decreased the drag coefficient by approximately 1%. However, significant length adjustment of the nose will cause another problem in the train's kinematics at the curved track.

The upper curve is directly related to the airflow smoothness from the nose to the transition area of the roof. An optimum design reduced the high-pressure region at the frontal area. The side curve of the HST acts as a flow diversion to the side. In addition, at the tail end, it helps weaken the wake vortices. Naturally, a sharp edge is favourable, but due to some mechanical and equipment arrangements, a wider edge is needed. Based on the simulation results, increasing the length and slenderness of the nose will improve the overall aerodynamic performance. However, the end decision of the optimum design is affected by design requirements such as interior capacity, equipment arrangement and other factors.

ACKNOWLEDGEMENT

REFERENCES

[1] X. Hu, Z. Deng, J. Zhang, and W. Zhang, "Aerodynamics behaviours in supersonic evacuated tube transportation with different train nose length," *Int. J. Heat Mass Transf.,* vol. 183(b), p. 122130, 2021.

[2] Z. Li, M. Yang, S. Huang, and D. Zhou, "A new mode test method for the measurement of aerodynamic drag coefficient of high-speed trains based on machine vision," *Proc. Inst. Mech. Eng. Pt. F. J. Rail Rapid Transit,* vol. 232, no. 5, pp. 1-12, 2017.

[3] Z. Sun, S. Yao, L. Wei, Y. Yao, and G. Yang, "Numerical investigation on the influence of the streamlined structures of the high-speed train's nose on aerodynamic performances," *Appl. Sci.*, vol. 11, no. 2, 2021.

[4] M. Kwak, S. Yun, and C. Park, "Optimal design for the nose shape of commercial high-speed train using function of train configuration," *J. Korean Soc. Railw.*, vol. 18, no. 4, pp. 279-288, 2015.

[5] J. Choi, K. Kim, "Effect of nose shape and tunnel cross-sectional area on aerodynamic drag of train traveling in tunnels," *Tunn. Undergr. Space Technol.*, vol. 41, pp. 62-73, 2014.

[6] H. Versteeg, and W. Malalasekera, *An Introduction of computational fluid dynamics, the finite volume method, second edition*. Pearson, 2007.

[7] C. Hirsch, *Numerical computation of internal &external flows, the fundamental of computational fluid dynamics, second edition.* Elsevier, 2007.

[8] CEN European Standard, "Railway Applications – Aerodynamics. Part 4: Requirements and Test Procedures for Aerodynamics on Open Track," CEN EN 14067-4, 2009.

[9] CEN European Standard, "Railway Applications – Aerodynamics. Part 6: Requirements and Test Procedures for Cross Wind Assessment," CEN EN 14067-6, 2010.

[10] J. Niu, Y. Wang, L. Zhang, and Y. Yuan, "Numerical analysis of aerodynamic characteristics of high-speed train with different train nose lengths," *Int. J. Heat Mass Transf.*, vol. 127(c), pp. 188-199, 2018.

[11] X. Li, G. Chen, D. Zhou, and Z. Chen, "Impact of different nose lengths on flow-field structure around a high-speed train." *Appl. Sci.*, vol. 9, no. 21, 2019.

[12] J. Mario, B. Halfina, D. Bahtera, L. Shalahuddin, and A. Windharto, "Numerical and experimental analysis of drag force in medium speed train design," *IOP Conf. Ser.: Mater. Sci. Eng.,* vol. 909, no. 1, p. 012031, 2020.

[13] S. Banga, M. Zunaid, N.A. Ansari, S. Sharma, and R.S. Dungriyal, "CFD simulation of flow around external vehicle: Ahmed Body," *IOSR J. Mech. Civ. Eng.,* vol 12, pp.87–94, 2015.

[14] J. Munoz-Paniagua, and J. García, "Aerodynamic drag optimization of a high-speed train," *J. Wind Eng. Ind. Aerodyn.*, vol. 204, p. 104215, 2020.